Comparison of OSIRIS stratospheric NO_2 and O_3 measurements with ground-based Fourier transform spectrometer measurements at the Toronto Atmospheric Observatory[1]

Jeffrey R. Taylor, Kimberly Strong, Chris A. McLinden, Douglas A. Degenstein, and Craig S. Haley

Abstract: Stratospheric NO_2 and O_3 retrieved from measurements of limb-scattered sunlight made by the Optical Spectrograph and InfraRed Imager System (OSIRIS) are compared with like observations made by a ground-based infrared Fourier Transform Spectrometer at the Toronto Atmospheric Observatory (TAO-FTS). Two different versions of OSIRIS NO_2 are compared (DOAS version 3.0 and MART version 2.0) with partial column concentrations retrieved from the TAO-FTS. Two OSIRIS O_3 versions are also compared (Triplet version 3.0 and MART version 2.0) with O_3 retrieved from the TAO-FTS. To accommodate the most coincidences, comparisons are based on monthly mean stratospheric partial columns covering 16–50 km. All coincident monthly means display high correlations: 0.82–0.97. The monthly mean NO_2 at TAO compared with the monthly mean NO_2 from OSIRIS shows an average difference of less than ~3% with standard deviations up to 6%. The OSIRIS NO_2 observations show a multiplicative bias of ~0.8–0.9 and a systematic difference of 5–10% greater then those of the TAO-FTS. O_3 differences are less than 5%, on average, with standard deviations ranging from 2% to 2.8%. There is a pronounced multiplicative bias of OSIRIS compared with the TAO-FTS ranging from 0.55 to 0.73. The systematic O_3 differences are less than 5% larger for OSIRIS. These small differences meet the standards outlined in the Integrated Global Observing Strategy and confirm the quality of the OSIRIS data for studying stratospheric ozone and nitrogen chemistry.

PACS Nos.: 92.60.hd, 92.60.Ry, 92.70.Cp, 93.30.Hf

Received 3 March 2007. Accepted 8 August 2007. Published on the NRC Research Press Web site at http://cjp.nrc.ca/ on 22 October 2007.

J.R. Taylor[2] and K. Strong. Department of Physics, University of Toronto, 60 St. George St., Toronto, ON M5S 1A7, Canada.
C.A. McLinden. Environment Canada, 4905 Dufferin St., Toronto, ON M3H 5T4, Canada.
D.A. Degenstein. Department of Physics and Engineering Physics, University of Saskatchewan, 116 Science Pl., Saskatoon, SK S7N 5E2, Canada.
C.S. Haley. Centre for Research in Earth and Space Science, York University, 4700 Keele St, Toronto, ON M3J 1P3, Canada.

[1]This original article is from work that highlights some of the science that has been produced in the last couple of years using the Odin satellite.

[2]Corresponding author (e-mail: jeff@atmosp.physics.utoronto.ca).

 doi: 10.1139/P07-144

Résumé : Les concentrations stratosphériques de NO_2 et de O_3, recouvrées des mesures de lumière solaire diffusée par le limbe terrestre à l'aide du spectrographe optique et de l'imageur infrarouge (OSIRIS), sont comparées avec des observations faites par le spectromètre infrarouge à transformée de Fourier de l'Observatoire Atmosphérique de Toronto (TAO-FTS). Les résultats de deux versions du code d'analyse OSIRIS NO_2 (DOAS v3.0 et MART v2,0) sont comparées avec des concentrations en colonnes partielles obtenues de TAO-FTS. Nous comparons aussi deux versions de OSIRIS O_3 (version triplet 3,0 et MART v2,0) avec les résultats de TAO-FTS. Afin d'améliorer le recouvrement des mesures, les comparaisons sont basées sur des moyennes mensuelles de colonnes stratosphériques partielles entre 16 et 50 km. Les moyennes mensuelles coïcindentes montrent un haut taux de corrélation de 0.82–0.97. La moyenne mensuelle du NO_2 au TAO comparée à la moyenne mensuelle de OSIRIS montre une différence moyenne de moins de 3 % avec un écart type de 6 %. Les observations NO_2 de OSIRIS montrent un biais multiplicatif de $\sim$0.8–0.9 et une différence systématique de 5–10 % plus grande que celles du TAO-FTS. Les différences systématiques des mesures de O_3 de OSIRIS sont plus grandes par moins de 5 %. Ces petites différences rencontrent les critères esquissés dans le Global Observing Strategy et confirment la qualité des données de OSIRIS dans l'étude de la chimie stratosphérique de l'ozone et du bioxyde d'azote.

[Traduit par la Rédaction]

1. Introduction

Ozone exists naturally in the stratosphere and much of its behaviour can be explained by the Chapman mechanism [1]. A more complete description requires stratospheric dynamics [2], which redistributes ozone from the tropics, where it is formed, to the mid-latitude and polar regions, as well as so-called catalytic destruction cycles involving oxides of hydrogen, nitrogen, chlorine, and bromine. In the middle stratosphere (25–40 km), catalytic destruction by NO_x (NO and NO_2) dominates [3–5]. Until 1997, mid-latitude O_3 in this region of the atmosphere was decreasing by about 6% per decade while it decreased by as much as 10–15% from 1979 to the 1990s [5]. The rate of decrease has since levelled off, while total column NO_2 is increasing by about 5.7–6.2% per decade [5, 6]. In addition to this direct role, NO_x is coupled to the hydrogen, chlorine, and bromine families and may form longer-lived "reservoir" species (for details, refer to Brasseur and Solomon [7]). To make accurate predictions about future concentrations of stratospheric ozone, measurements must be at least as precise as these trend estimates. According to the requirements established for the Integrated Global Observing Strategy of the European Space Agency, lower stratospheric O_3 observations should be accurate to within 5% of the truth with a threshold of 20%, while lower stratospheric NO_2 observations should be accurate to within 15% of the truth with a threshold of 40% [8].

Fourier Transform InfraRed (FTIR) spectroscopy has been utilized as an effective technique for remote sensing of the atmosphere for over 40 years [9]. Since January 1991, high-resolution ground-based Fourier Transform Spectrometers (FTSs) have been used for atmospheric remote sensing by recording infrared solar absorption spectra under the auspices of the Network for the Detection of Atmospheric Composition Change (NDACC), (formerly known as the Network for the Detection of Stratospheric Change-NDSC) [10]. These observations provide trace gas concentrations in the stratosphere and troposphere for use in trend and climate studies, for example, refs. 11–13 as well as for correlative ground-truthing of space-based observations, for example, refs. 14–17.

In 2001, the Toronto Atmospheric Observatory was established with a high-resolution ground-based FTS as its principal instrument (TAO-FTS). Currently, it is one of only two such NDACC instruments operating in Canada and has been used for both ground-truthing [18, 19] and scientific process studies [20].

The Optical Spectrograph and InfraRed Imager System (OSIRIS) [21] is one of two instruments that were launched on board the Odin Satellite in February 2001 [22]. This Canadian instrument is designed

to record atmospheric extinction spectra in the ultraviolet/visible from limb-scattered sunlight. This technique allows for both global coverage and relatively high vertical resolution, yielding vertical profiles of trace gas concentrations from approximately 12–50 km altitude [23, 24]. OSIRIS NO_2 and O_3 data sets have been validated with coincident satellite and sonde observations [25–27]. These data have, in turn, served as the calibrated "truth" for validating other atmospheric measurements [28].

This intercomparison seeks to provide the first statistical ground-truthing of OSIRIS observations with the latest version (v3.0) of O_3 and NO_2 observations by OSIRIS [29] with like measurements from the TAO-FTS. It will also provide the first comparison with retrievals made by the OSIRIS MART Algorithm. The coincident data that have been recorded for more than 4 years provides an opportunity not only to investigate simple observation biases, but also to statistically investigate issues related to temporal coincidence. The effects of comparing an infrared observing system with that of a UV/visible instrument are also addressed by comparing differing retrieval techniques.

2. Instruments and retrieval methodology

2.1. TAO-FTS

The Toronto Atmospheric Observatory (43° 40′N, 79° 24′ W, 174.0 m above sea level) was established in 2001 with the installation of a high-resolution, DA8-model infrared Fourier Transform Spectrometer manufactured by ABB Analytical Business PRU (formerly Bomem Inc.), Québec, Canada. The optical design of the instrument consists of a vertically oriented, linear Michelson interferometer with a maximum optical path difference (OPD) of 250 cm, providing a maximum unapodized resolution of 0.004 cm^{-1}. This design incorporates a novel dynamic alignment that is described in detail by Wiacek et al. [30].

Infrared solar absorption spectra are regularly recorded with indium antimonide (InSb) and mercury cadmium tellurium (MCT) detectors using a potassium bromide (KBr) beamsplitter to cover the range 750–4400 cm^{-1}. All of the internal optics, including the liquid-nitrogen-cooled detectors, are evacuated to approximately 0.06 Torr (1 Torr = 133.3223 Pa). The external optical components include a dedicated altitude-azimuth tracker (manufactured by AIM Controls Inc., Calif. USA) which actively tracks direct solar radiation throughout the day, as well as several flat mirrors and a collimating mirror used to direct the radiation into the interferometer with a full field of view of approximately 1.54 mrad (with the InSb detector). Clear-sky conditions are necessary to acquire solar spectra, restricting the average number of observing days to approximately 90 per year over the first 4 years of operation. The TAO-FTS has been routinely gathering spectra since May 2002.

Spectra are recorded by using six different narrow-band optical interference filters that are widely used within the NDACC InfraRed Working Group (IRWG). For the purposes of this comparison, only measurements from one of these filters is used with the InSb detector, reducing the spectral range to 2400–3100 cm^{-1}. To attain a higher signal-to-noise ratio (SNR), each interferogram consisted of four co-added, 250 cm optical path difference scans recorded in the forward direction, resulting in one spectrum attained over a period of approximately 20 min. Each interferogram was transformed into a spectrum using a boxcar apodization function.

The TAO-FTS NO_2 retrievals were calculated with the SFIT2 retrieval algorithm (v3.82beta3) [31, 32] using spectral parameters from the HITRAN 2004 database [33]. This algorithm utilizes the Optimal Estimation Method (OEM) that is commonly employed in deriving vertical profiles of atmospheric trace gases from ground-based solar absorption spectra. A rigorous derivation of the mathematical formalism relevant to this technique can be found in Rodgers [34].

To adequately characterize the a posteriori state, the retrieved best estimate, $\hat{\boldsymbol{x}}$, can be regarded as a combination of an a priori estimate of the atmospheric state, $\boldsymbol{x}_a$, and the true atmospheric state, $\boldsymbol{x}$

$$\hat{\boldsymbol{x}} = \boldsymbol{x}_a + \boldsymbol{A}\,(\boldsymbol{x} - \boldsymbol{x}_a) + \epsilon \tag{1}$$

where ϵ is the error, and $\boldsymbol{A}$ is known as the averaging kernel matrix, which represents the sensitivity of the retrieved state to the true state.

The NO_2 fits were performed on the $\nu_1 + \nu_3$ vibrational–rotational band in a microwindow from 2914.59 to 2914.70 cm^{-1}, which was first investigated by Camy-Peyret et al. [35]. A volume-mixing-ratio profile retrieval was performed, with the trace gas of interest represented on a 38 layer altitude grid in the retrieved state space. Spectroscopically interfering species (in this case, CH_4 and H_2O) were considered by determining the scaling factors that result in the best overall spectral fit when applied to the entire a priori profile of each interfering gas. Column concentrations retrieved with SFIT2 from ground-based spectra have been compared with like results from other retrieval algorithms and have been found to agree within 1% for matched retrieval constraints [36]. NO_2 has been previously measured with ground-based FTIR spectroscopy, see, for example, refs. 17, 37–40 and has been characterized at TAO. The a priori profile was constructed from a 15 year climatology of HALogen Occultation Experiment (HALOE) data (v.19) between 19–44 km [41], with the remainder of the profile constructed from Michelson Interferometer for Passive Atmospheric Sounding (MIPAS) mid-latitude daytime reference climatology profiles (v.3.0) [42]. The a priori error estimates used here were set to 40% between 1055 km and tapered to 10% outside of this region (for a detailed description of these NO_2 retrievals, refer to ref. 43). The retrievals resulted in a mean total column degrees-of-freedom for signal of 1.6, with the sensitivity concentrated primarily in the stratosphere (see Sect. 3).

O_3 measurements recorded by ground-based infrared Fourier transform spectroscopy have been previously used to validate similar measurements from satellites, see, for example, refs. 44, 45. Like NO_2, O_3 measurements have been made at TAO since May 2002 and have been previously characterized using the SFIT2 profile retrieval algorithm (for details of the retrieval characteristics, refer to ref. 43). The chosen microwindow has been used in previous intercomparison exercises and has proven useful for identifying differences in retrievals [46]. It was composed of multiple band passes in the the $2\nu_1 + \nu_2$ band: 2775.68–2776.30 cm^{-1}, 2778.85–2779.20 cm^{-1}, and 2781.57–2782.06 cm^{-1}. These three band passes were fitted simultaneously with interfering species CH_4, H_2O, HDO, CO_2, HCl, and N_2O so as to achieve the best global fit. This resulted in a mean total column degrees-of-freedom for signal of 2.1. As with NO_2, all of these retrievals were completed on a 38 layer altitude grid using an a priori profile constructed from HALOE and MIPAS climatologies. The a priori covariance matrix was set to 20% over the entire altitude range.

2.2. OSIRIS

The Odin satellite is in a Sun-synchronous orbit at 600 km with the ascending node at 18 h Local Solar Time and carries two instruments dedicated to two mission goals; OSIRIS exclusively carries out aeronomy studies while the Sub-millimetre and Millimetre Radiometer (SMR) [47] records both astronomical and aeronomical observations. The Optical Spectrograph (OS) uses a grating spectrometer and an EEV Charge Coupled Device to record spectra of Rayleigh-scattered sunlight along the limb within the wavelength range 280–800 nm with 1 nm resolution [21]. This provides vertical profile concentrations of several atmospheric trace gases, including O_3 and NO_2, as well as BrO, OClO and aerosols. A complete stratospheric scan requires about 85 s and hemispheric coverage is obtained through most of the year, with global coverage at the equinoxes. Because Odin is a two-discipline satellite, measurement time is divided such that the stratospheric observation mode happens one out of every three days [48].

NO_2 profiles were retrieved from the OSIRIS limb-scattered sunlight measurements using two different techniques. The first technique utilized a Differential Optical Absorption Spectroscopy (DOAS) algorithm with a maximum a posteriori estimator [23]. The fitted spectral microwindow ranged from 435 to 451 nm, with O_3 and O_4 fitted as interfering species. These measurements nominally cover a tangent height altitude range of 10–70 km with regular extensions up to 100 km altitude and a vertical resolution of roughly 2 km. A previous version of level 2 data retrieved with this algorithm compared well with

like observations from other satellite platforms [25]. Version 3.0 of the OSIRIS-DOAS NO_2 data set has been used in this study [29]. The second technique was developed at the University of Saskatchewan and uses retrieval algorithms based upon a Multiplicative Algebraic Reconstruction Technique (MART) [49]. This algorithm uses a maximum likelihood expectation estimator over a narrower wavelength region, while simultaneously fitting aerosol concentrations. This comparison will provide the first validation of the NO_2 data products produced by the version 2.0 MART retrieval.

The OSIRIS O_3 retrievals were again carried out using two different techniques. The first used the so-called Triplet Algorithm (version 3.0) to retrieve O_3 vertical profiles from the Chappuis absorption band [24, 29, 50]. This technique uses the ratio of limb radiances at three different wavelengths (602.0, 540.2, and 663.9 nm) with Optimal Estimation to determine the altitude distribution of O_3. The second technique used the same MART retrieval that was used for NO_2 retrievals (version 2.0) [49]. The O_3 MART retrieval not only relied on the Chappuis absorption band, but also included measurements from the Huggins band. This should provide greater sensitivity to ozone at higher altitudes (although, for consistency, the same altitude regions will be compared for all retrievals). As with NO_2, these measurements had a vertical resolution of roughly 2 km.

3. Analysis and results

3.1. NO_2 comparisons

As has been used in previous OSIRIS validation studies [28], the spatial coincidence selection criterion was chosen to be within $\pm 5°$ latitude and $\pm 10°$ longitude of TAO (that is, all coincidences are within ± 1000 km of TAO). Other comparisons of ground-based NO_2 observations as with satellite observations utilize a spatial coincidence criteria of 750 km [51]. A slightly broader definition was chosen for this study so as to maximize the number of comparable observations.

The high degree of spatial coverage of OSIRIS resulted in 904 coincident observations between May 2002 and December 2006. Throughout this same time period, the TAO-FTS recorded 567 measurements. However, due to the orbit of Odin, OSIRIS observations are limited in the winter hemisphere, effectively restricting coincidence to March through October. This large number of spatially coincident measurements reduces sampling problems that often inhibit rigorous statistical comparisons from being made between two differing observation platforms. However, it is important to note that the short lifetime of NO_2 (see Sect. 1) necessitates a strict temporal coincidence criterion for comparing individual measurements.

Following the approach first proposed by Sussmann et al. at the Zugspitze Ground-Truthing Facility [17], the TAO NO_2 columns were corrected using "virtual coincidences". Previous corrections for NO_2 temporal coincidence have been made with photochemical box models, see, for example, ref. 52, but the errors associated with this technique are difficult to estimate [53]. The virtual coincidence technique relies on the fact that there is no significant seasonal dependence in the daytime rate of increase of NO_2 at mid-latitudes. The annual average daytime increasing rate of 1.02×10^{14} molecules/(cm^2/h) found at Zugspitze (47.42°N, 10.98°E) should be representative of that of Toronto (43.66°N, 79.40°W). Furthermore, error estimates can be made by using the difference in time between coincident measurements.

For each day of individual measurements recorded in Toronto, the NO_2 daily growth rate is used for extrapolating concentrations to coincide with the time of the OSIRIS overpass. By fitting a straight line with a constant slope 1.02×10^{14} (i.e. only allowing the vertical offset for this trend line to be fit) to the TAO NO_2 columns, these "virtual coincidences" can be defined (an example is shown in Fig. 1). Since the error in the daytime increasing rate is 0.06×10^{14} molecules/(cm^2/h) [17], this value can simply be multiplied by the number of hours separating the measurements to yield a conservative error estimate. To further mitigate temporal-sampling problems, the data were sorted into monthly bins and monthly mean statistics were calculated from each instruments' data. Only months in which each instrument had recorded more than five measurements were used for comparison (see Fig. 2).

Fig. 1. "Virtual coincidence" correction of NO_2 partial columns measured at TAO on 1 September 2005. The slope of 1.02 $\times 10^{14}$ molecules/(cm^2/h) was fixed for each day and only the vertical offset was fitted to the retrieved columns. The "coincidences" are extrapolated from the slope so as to coincide with the times of the OSIRIS overpass.

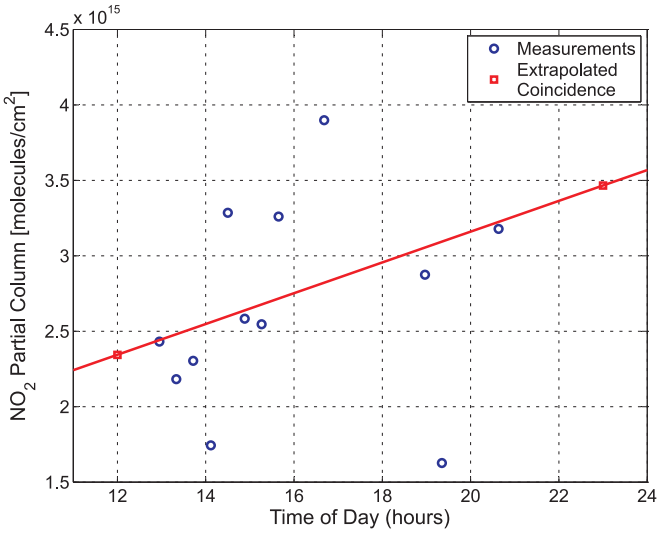

Fig. 2. Monthly observation frequency of AM and PM measurements recorded by the TAO-FTS and OSIRIS from May 2002–December 2006. The broken line represents the minimum statistical limit of five measurements; any month in which either instrument has fewer measurements is not used for this comparison.

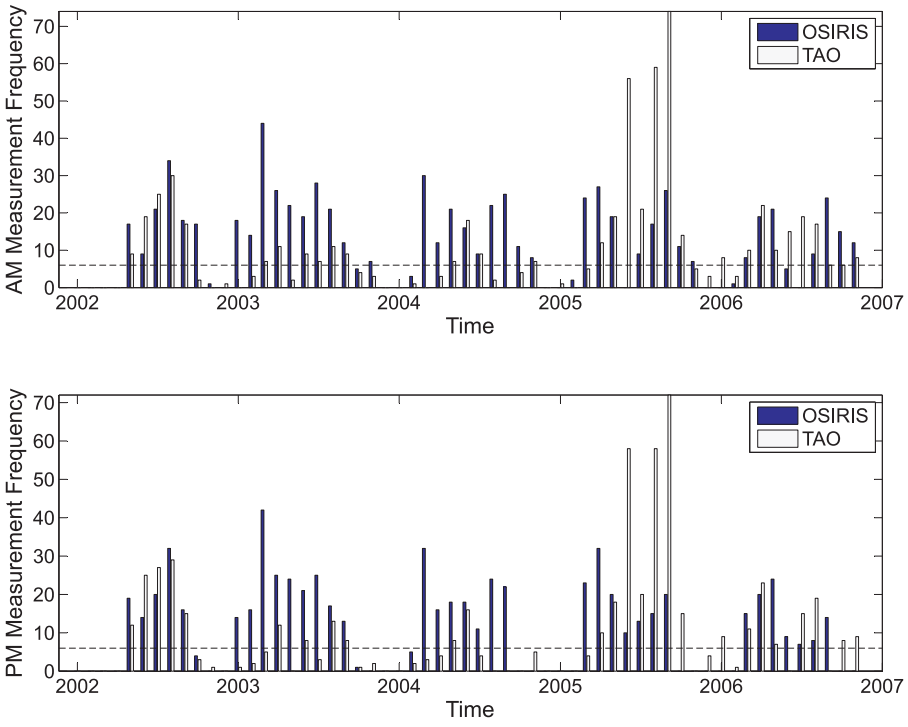

Fig. 3. (*a*) NO_2 partial column averaging kernel for the TAO-FTS. This represents the altitude sensitivity of the measurement to atmospheric concentrations between 16–50 km. (*b*) O_3 partial column averaging kernels for the TAO-FTS, representing sensitivity over the same altitude range.

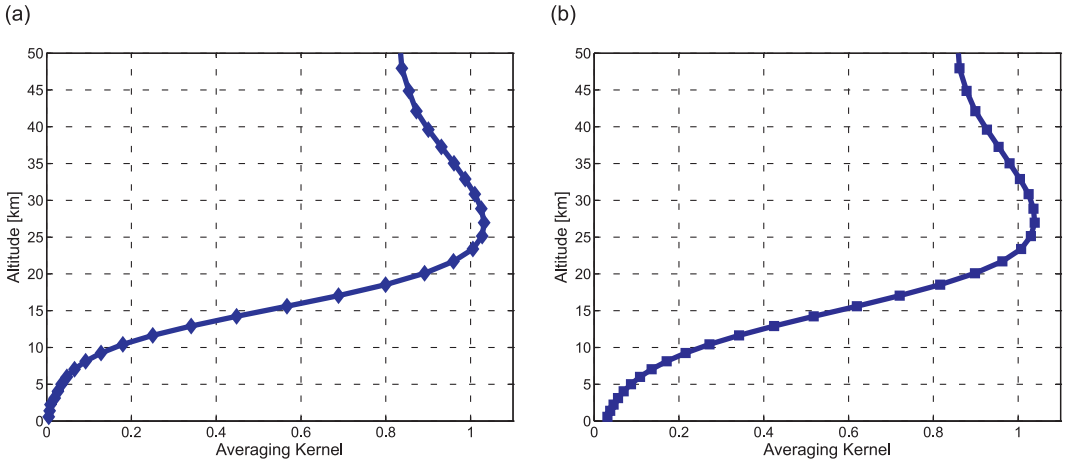

Fig. 4. Time series of monthly mean NO_2 partial columns for each month in which there are more than five measurements. Triangles represent the DOAS-based retrievals from OSIRIS, circles represent the MART-based retrievals from OSIRIS, and diamonds represent the values derived from the TAO-FTS. Error bars show one standard deviation.

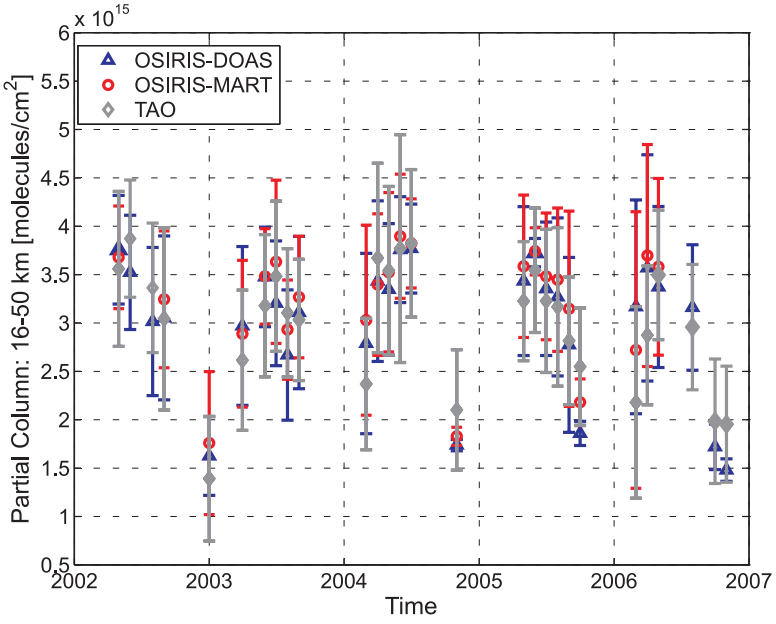

To ensure that the peak stratospheric concentrations were captured for the comparison, partial columns were integrated between 16–50 km, yielding 1.4 degrees-of-freedom for signal. Since the TAO-FTS retrieves vertical information with a coarser vertical resolution than OSIRIS, the TAO-FTS averaging kernels (see Fig. 3*a*) were used for smoothing and integrating the OSIRIS profiles into partial columns. Equation (1) is used to do this, but here $\boldsymbol{x}$ is the original OSIRIS profile and $\hat{\boldsymbol{x}}$ is the smoothed profile. For details of this technique, refer to ref. 54.

Figure 4 shows the monthly mean time series of all three NO_2 data products. Although the individual monthly means display close agreement, it is necessary to consider long-term biases for data sets of this length. From the scatter plot shown in Fig. 5*a*, it may be seen that the OSIRIS-MART data and the TAO-FTS data have a high correlation (correlation coefficient = 0.89) with apparently random differences. The weighted least-squares linear fit to the scatter plot shows a slope of 0.92, indicating that there is a multiplicative bias favouring the MART retrievals, that is, for larger column concentrations, the MART retrieval captures slightly elevated concentrations of NO_2 while for smaller column concentrations, the TAO-FTS shows relatively higher columns. Although no systematic bias is readily evident from the scatter plot, Fig. 5*b* shows that the differences between the columns are evenly distributed, but slightly biased to higher MART columns suggesting a systematic difference of approximately 10%.

Comparisons between the OSIRIS-DOAS retrievals and the TAO-FTS yield similar results (Figs. 5*c*–5*d*). The data have a correlation of 0.85, and the linear fit to the scatter plot also shows a multiplicative bias that favours the OSIRIS columns (slope = 0.79). The histogram in Fig. 5*d* shows that the OSIRIS-DOAS data exhibit, on average, a small systematic difference of 5% over that of the TAO monthly means.

The two OSIRIS retrieval techniques also show some differences (Figs. 5*e*–5*f*). As should be expected of two differing retrievals from the same data, the correlation is high (0.93), but the scatter plot shows a slight multiplicative bias. The linear fit to the scattered data has a slope of 0.87, indicating that the DOAS retrieval captures slightly higher monthly mean columns than those of the MART retrieval. Furthermore, the histogram shows that the DOAS retrievals have an average systematic bias of approximately 5% over MART.

Previous comparisons between NO_2 observations made in the UV–visible have shown that differences in absorption cross sections can generate as much as 5% systematic disagreement among columns [55]. In this comparison, DOAS and MART retrievals used UV–visible cross sections from Vandaele et al. [56], while the TAO NO_2 retrievals used infrared parameters originally published by Perrin et al. [57]. Since this comparison is obviously relying on differing spectroscopic parameterization between the infrared and UV–visible, it is unrealistic to expect that columns should agree to better than this 5% limit. The comparison between the two OSIRIS retrievals reveal a general systematic difference evenly distributed around 5%. Similarly, the DOAS and TAO NO_2 differences are close to 5%. Only the MART−TAO difference shows a distribution around 5%–10%, suggesting that these two data sets have a systematic bias that may be greater than any spectroscopically induced bias. As this is the first validation of products generated by the MART retrieval algorithm, it is possible that this systematic bias is a direct result of the retrieval. However, previous profile-based comparisons of OSIRIS NO_2 (version 2.4) with like measurements from an infrared instrument (HALOE) that have shown that OSIRIS generally reports higher values above 35 km [25] and the column discrepancy observed here may be a manifestation of this difference.

3.2. O_3 comparisons

The same temporal and spatial coincidence criteria were used for selecting OSIRIS O_3 measurements. This resulted in 904 coincident OSIRIS observations and 651 TAO-FTS observations of O_3 between May 2002 and December 2006. The data were sorted into monthly bins to facilitate monthly mean comparisons. Unlike NO_2, the distribution of temporal sampling within a month is not problematic as the lifetime of O_3 at 30 km altitude is on the order of weeks [7]. Therefore, monthly mean values should be representative of the true stratospheric O_3 concentration. However, to maintain consistency, the same minimum sample criterion of five measurements per instrument per month was implemented.

Figure 6 shows the complete time series of monthly mean O_3 partial columns produced by each of the three retrievals. With the exception of some obvious discrepancies at the beginning of 2003, most mean values agree to within 1σ. The relatively long lifetime of O_3 also acts to reduce the amount of scatter within a given month, resulting in significantly smaller 1σ standard deviations than those of NO_2

Fig. 5. (*a*) NO_2 monthly means derived from TAO-FTS observations scatter plotted against monthly means derived from OSIRIS-MART retrievals. Error-bars represent one standard deviation. The continuous line shows the 1:1 line and the broken line shows a weighted-least-squares linear fit to the data. (*b*) Histogram of the differences between monthly mean partial columns: 100*2*(MART - TAO)/(MART + TAO). (*c*) Same as (*a*), but comparing TAO-FTS monthly means with those of OSIRIS-DOAS retrievals. (*d*) Histogram of the differences between monthly mean partial columns: 100*2*(DOAS-TAO)/(DOAS + TAO). (*e*) Same as (*a*), but comparing OSIRIS-MART monthly means with those of OSIRIS-DOAS retrievals. (*f*) Histogram of the differences between monthly mean partial columns: 100*2*(DOAS - MART)/(DOAS + MART).

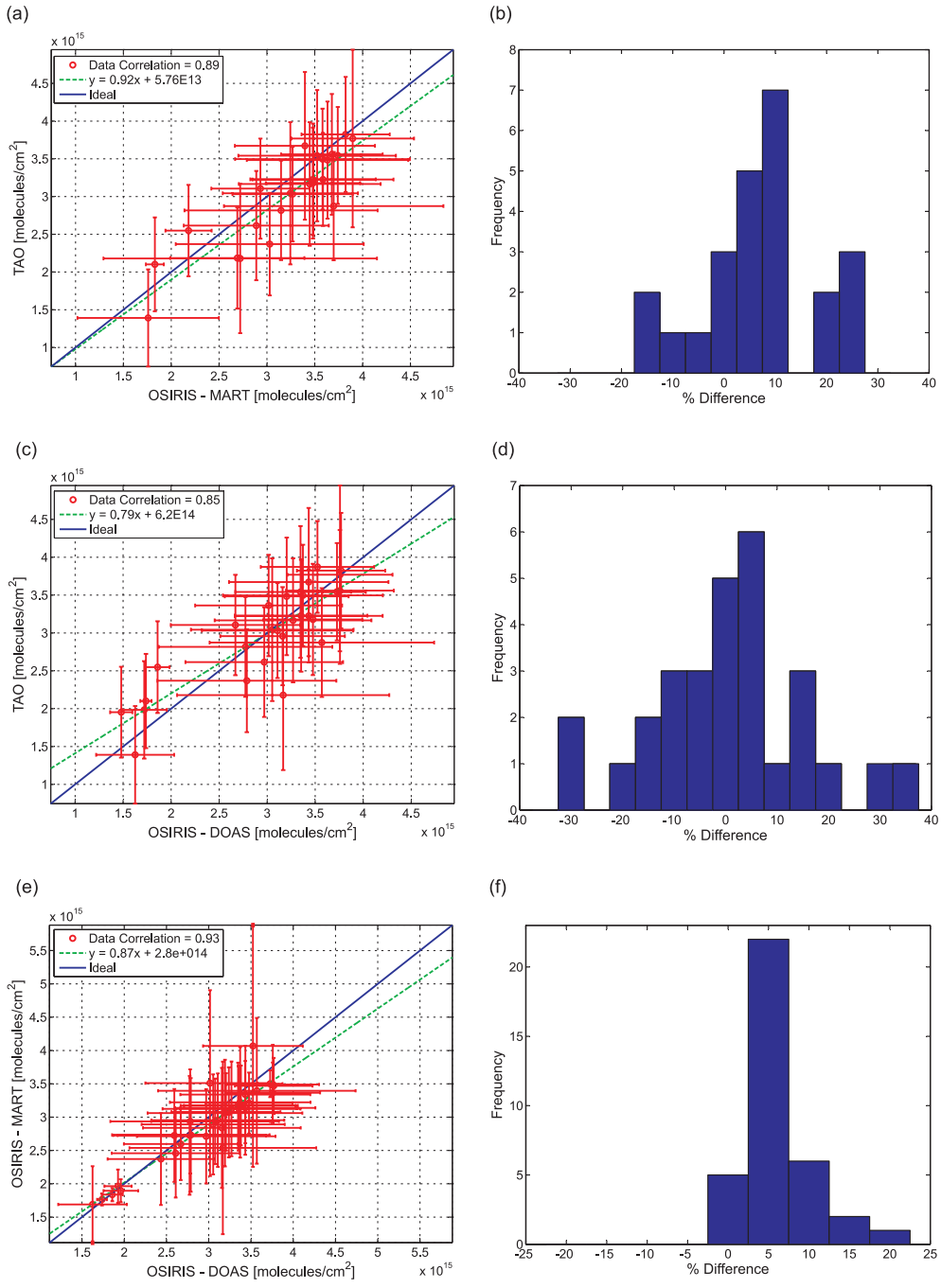

Fig. 6. Time series of monthly mean O_3 partial column concentrations for each month in which there are more than five measurements. Triangles represent the Triplet-based retrievals from OSIRIS, circles represent the MART-based retrievals from OSIRIS, and diamond symbols show values from the TAO-FTS. Error bars show one standard deviation.

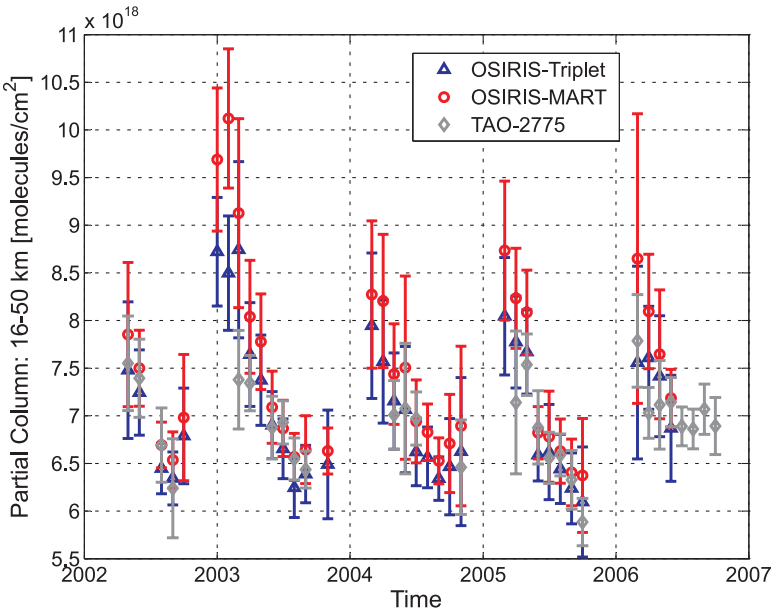

(see Fig. 4). Again, the apparent individual agreement for most months does not preclude the chance of inherent bias between data sets.

The OSIRIS-MART O_3 retrievals are compared with the TAO-FTS O_3 data set in Fig. 7*a*. To minimize the errors arising from the differences in altitude sensitivity of the two observing systems, the OSIRIS profiles were smoothed with the TAO-FTS O_3 averaging kernels and integrated into partial columns from 16–50 km altitude (see Fig. 3*b*). The TAO retrievals show good correlations with the MART monthly means (0.84) however, the linear fit to the scatter plotted data has a slope much less than 1 (0.55). This once again indicates that the MART retrievals have a relative multiplicative bias that results in generally capturing higher O_3 monthly mean values for months in which the concentration is higher, and the TAO-FTS retrievals show mainly higher values from months in which the O_3 concentration is lower. However, the histograms indicate that the systematic differences between the data sets are less conclusive. Comparing the TAO monthly means with those of the MART retrievals (Fig. 7*b*) shows that the MART data, in general, are skewed to retrieve 5% higher values and have some differences that are as large as 20%.

Making these same comparisons with the OSIRIS-Triplet retrievals shows slightly different results. Figure 7*c* and 7*d* show the scatter plots between the TAO and OSIRIS-Triplet monthly means. Once again, the data show a strong correlation (0.82) and the slope of the linear fit is less than 1 (0.73). This suggests that the Triplet-based O_3 means have a multiplicative bias that is similar to that of the MART-based means (albeit, not as strong). However, a systematic bias is not suggested by the histogram (Fig. 7*d*). The mean comparison shows a distribution of differences centred around 0% while there is a small number of outlying higher concentrations recorded at TAO.

Comparing the two OSIRIS retrieval techniques also identifies a bias (Fig. 7*e*–7*f*). There are both systematic biases and multiplicative biases that favour the MART-based retrieval. From the scatter plots shown in Fig. 7*e*, the slope of the linear fit is 1.3, illustrating a clear multiplicative bias of higher monthly

Fig. 7. (*a*) O_3 monthly mean partial columns derived from TAO-FTS observations plotted against monthly means derived from OSIRIS-MART retrievals. Error bars represent one standard deviation. The continuous line shows the 1:1 line and the broken line shows a weighted-least-squares linear fit to the data. (*b*) Histogram of the differences between monthly mean partial columns: 100*2*(MART – TAO)/(MART + TAO). (*c*) Same as (*a*), but comparing TAO-FTS monthly means with those of OSIRIS-Triplet retrievals. (*d*) Histogram of the differences between monthly mean partial columns: 100*2*(Trip. – TAO)/(Trip. + TAO). (*e*) Same as (*a*), but comparing OSIRIS-MART monthly means with those of OSIRIS-Triplet retrievals. (*f*) Histogram of the differences between monthly mean partial columns: 100*2*(Trip. – MART)/(Trip. + MART).

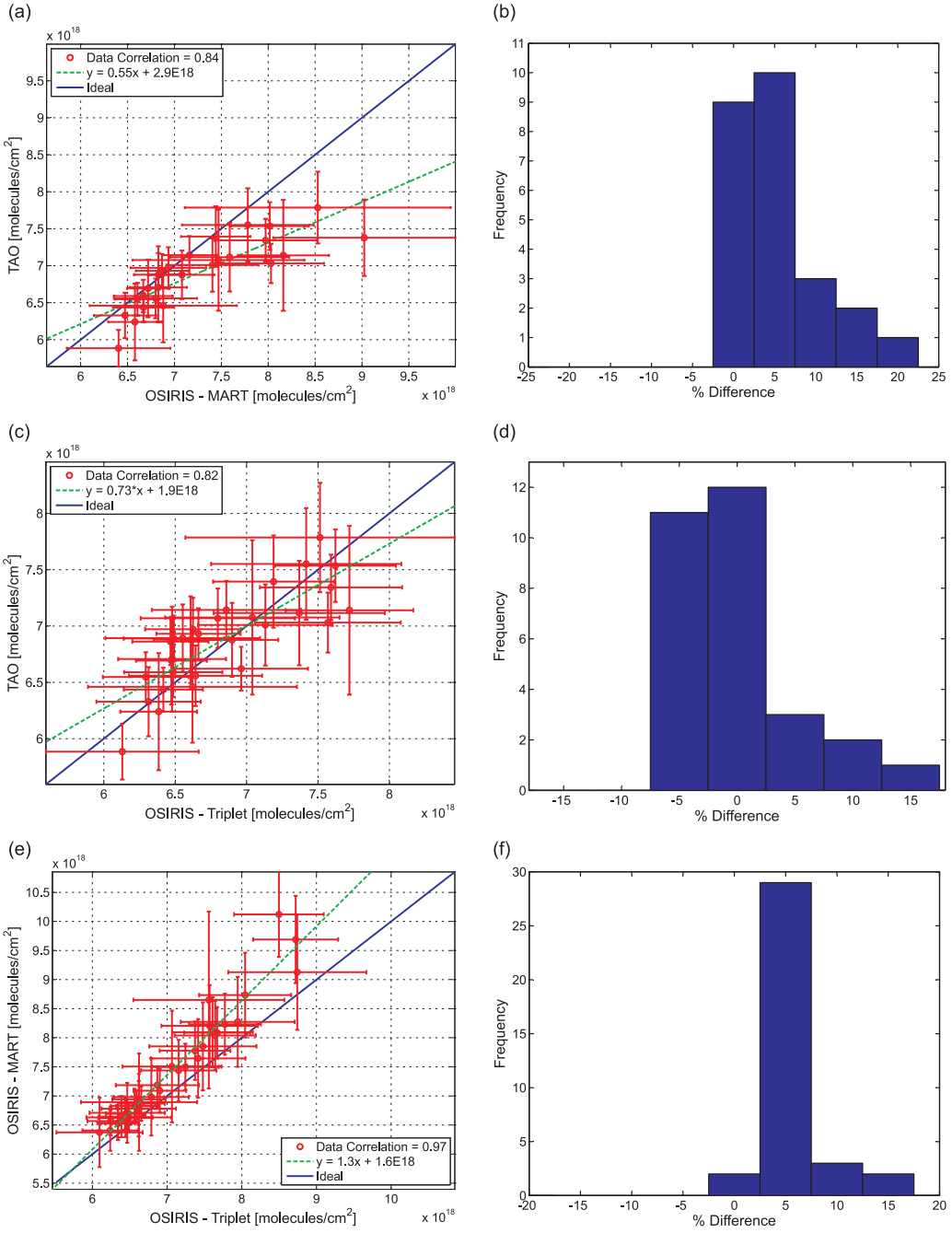

Table 1. Statistics of OSIRIS − TAO monthly mean column amounts. The comparison denotes the two retrieval methods being compared (the first minus the second). Number of months compared: n. Calculated correlation coefficient: R^2. Mean percent difference in monthly mean column amounts: $\overline{\delta}$. Standard deviation of the mean percent difference in monthly mean column amounts: σ_δ. Calculated slope of the linear weighted-least-squares fit to the scatter plots of the first retrieval versus the second retrieval. The value of the strongest statistical mode present in the histogram of the percent differences.

Comparison	n	R^2	$\overline{\delta}$ (%)	σ_δ (%)	slope	mode (%)
NO_2 (MART − TAO)	22	0.89	+3.1	1.7	0.92	+10
NO_2 (DOAS − TAO)	29	0.85	+0.1	6.0	0.79	+5
NO_2 (DOAS − MART)	36	0.93	+1.9	3.6	0.87	+5
O_3 (MART − TAO)	25	0.84	+2.5	2.8	0.55	+5
O_3 (Trip. − TAO)	29	0.82	−0.3	2.0	0.73	0
O_3 (Trip. − MART)	36	0.97	−2.6	2.0	1.3	+5

means from the MART data. These same data values are systematically 5% greater than those derived from the Triplet-based retrieval. A similar systematic bias of 5% was seen between the two OSIRIS NO_2 retrievals.

Previous comparisons of ground-based O_3 measurements by infrared FTS with those of the UV–visible satellite SCIAMACHY (SCanning Imaging Absorption spectroMeter for Atmospheric CHartographY) have been shown to deviate significantly in the stratosphere, with the FTS values consistently lower than those of the satellite [58]. For both OSIRIS retrievals, all O_3 cross sections were taken from Bogumil et al. [59], while the HITRAN 2004 infrared line parameters were based on original work by Mikhailenho et al. [60] and De Backer-Barilly et al. [61]. Validation of the ACE-FTS satellite instrument has included comparisons of O_3 profiles derived from infrared measurements with profiles from OSIRIS retrieved using the previous version of the Triplet algorithm [28]. This comparison showed that there can be differences as large as 30% at some altitudes. Previous UV–visible satellite comparisons have also shown that OSIRIS regularly underestimates O_3 above 40 km [26]. The MART comparisons do not seem to replicate this underestimation at higher altitudes (possibly due to the inclusion of the Huggins band in the retrieval algorithm). Although integration into partial columns should reduce differences arising from altitude sensitivity, these previously identified differences appear to be consistent with the TAO comparisons.

4. Conclusions

Stratospheric NO_2 and O_3 columns measured by the OSIRIS satellite instrument from May 2002–December 2006 were compared with like measurements from a ground-based Fourier transform spectrometer located at the Toronto Atmospheric Observatory. NO_2 profiles were retrieved from OSIRIS UV–visible limb-scatter measurements using both DOAS and MART retrieval algorithms. OSIRIS O_3 profiles were derived from the MART algorithm as well as with the Triplet retrieval method. The TAO-FTS partial columns were retrieved with the SFIT2 optimal estimation algorithm. All coincidences were confined to be within 1000 km of the TAO-FTS, with like measurements sorted into monthly bins to derive mean partial column concentrations from 16–50 km.

The NO_2 comparisons used coincident data spanning 59 months (see Table 1 for details). All three comparisons showed a high degree of correlation, ranging from 0.85 to 0.93 and had a mean difference that ranged from 3% for OSIRIS-MART versus TAO down to nearly 0% for OSIRIS-DOAS versus TAO. The standard deviations of these differences were less than 6.0%. Of the two OSIRIS retrievals,

the DOAS retreival showed a marked systematic bias of 5% greater than the MART retrieval. The agreement between OSIRIS-MART and TAO and OSIRIS-DOAS and TAO are as good or better than previous NO_2 column comparisons between infrared and UV–visible instruments.

The O_3 coincident comparisons spanned 58 months and also displayed well-correlated monthly means (0.82–0.97). The mean differences were +2.5%, −0.3%, and −2.6% for MART-TAO, Triplet-TAO, and Triplet-MART, respectively, with standard deviations all less than 3%. The apparent high bias for the OSIRIS-MART values may be generated by the higher altitude sensitivity caused by the inclusion of the Huggins band in the MART retrievals. There were definite multiplicative biases between some data sets (OSIRIS-MART and TAO), as well as systematic differences.

These two latest versions of OSIRIS retrievals for both O_3 and NO_2 have been shown to agree well with like observations from a ground-based Fourier transform spectrometer in Toronto. The OSIRIS observations provide global coverage and are of value for the continued monitoring of stratospheric O_3 chemistry as well as for predicting future trends.

Acknowledgments

The authors wish to thank A. Wiacek, T. Kerzenmacher, R. Lindenmaier, R. Batchelor, M. Wolff, D. Edwards, G. Hassanpour, M. Jensen, O. Mikhailov, K. MacQuarrie and R. Saari for their technical support and help with measurements. Funding for this work was provided by the Natural Sciences and Engineering Research Council, the Canadian Space Agency, the Canadian Foundation for Climate and Atmospheric Sciences, ABB Bomem, the Canadian Foundation for Innovation, the Ontario Research and Development Challenge Fund, the Premier's Research Excellence Award, and the University of Toronto.

References

1. S. Chapman. Philos. Mag. **10**, 369 (1930).
2. L.L. Hood and B.E. Soukharev. J. Atmos. Sci. **62**, 3724 (2005).
3. P.J. Crutzen. Q. J. R. Meteorol. Soc. **96**, 320 (1970).
4. P.J. Crutzen. J. Geophys. Res. **76**, 7311 (1971).
5. WMO (World Meteorological Organization). Scientific assessment of ozone depletion: 2006, global ozone research and monitoring project. Report No. 50. Technical Report, Geneva, Switzerland. 2007.
6. J.B. Liley, P.V. Johnston, R.L. McKenzie, A.J. Thomas, I.S. Boyd. J. Geophys. Res. **105**, 11633 (2000).
7. G. Brasseur and S. Solomon. Aeronomy of the middle atmosphere. 2nd ed. D. Reidel Publishing Company, Dordrecht. 1986.
8. IGOS (Integrated Global Observing Strategy). The changing atmosphere: An integrated global atmospheric chemistry observation theme for the IGOS partnership – GAW. Report No. 159. Geneva, Switzerland. 2004.
9. J. Connes. Revue d'Optique, **40**, 45 (1961).
10. M.J. Kurylo and R.J. Zander. *In* Proceedings of the 19th Quadrennial Ozone Symposium, Sapporo, Japan. July 2000. International Ozone Commission, Hokkaido, Japan. 2000.
11. C.P. Rinsland, A. Goldman, E. Mahieu, R. Zander, L.S. Chiou, J.W. Hannigan, S.W. Wood, and J.W. Elkins. J. Quant. Spectros. Radiat. Transfer, **92**, 201 (2005).
12. C.P. Rinsland, A. Goldman, J.W. Elkins, L.S. Chiou, J.W. Hannigan, S.W. Wood, E. Mahieu, and R. Zander. J. Quant. Spectros. Radiat. Transfer, **97**, 457 (2006).
13. J.W. Hannigan, M.T. Coffee, M.G. Mankin, and A. Goldman. J. Atmos. Chem. **30**, 103 (1998).
14. A. Griesfeller, J. Griesfeller, F. Hase, I. Kramer, P. Loës, S. Mikuteit, U. Raffalski, T. Blumenstock, and H. Nakajima. J. Geophys. Res. **111**, D11S07 (2006); doi:10.1029/2005JD006451.
15. R. Sussmann and M. Buchwitz. Atmos. Chem. Phys. **5**, 1497 (2005).
16. R. Sussmann, W. Stremme, M. Buchwitz, and R. de Beek. Atmos. Chem. Phys.**5**, 2419 (2005).
17. R. Sussmann, W. Stremme, J.P. Burrows, A. Richter, W. Seiler, and M. Rettinger. Atmos. Chem. Phys. **5**, 2657 (2005).

18. E. Mahieu, R. Zander, P. Duchatelet, J.W. Hannigan, M.T. Coffey, S. Mikuteit, F. Hase, T. Blumenstock, A. Wiacek, K. Strong, J.R. Taylor, R. Mittermeier, H. Fast, C.D. Boone, S.D. McLeod, K.A. Walker, P.F. Bernath, C.P. Rinsland. Geophys. Res. Lett. **32**, L15S08 (2005); doi:10.1029/2005GL022396.
19. B. Dils, M. De Mazière, T. Blumenstock, M. Buchwitz, R. de Beek, P. Demoulin, P. Duchatelet, H. Fast, C. Frankenberg, A. Gloudemans, D. Griffith, N. Jones, T. Kerzenmacher, I. Kramer, E. Mahieu, J. Mellqvist, R.L. Mittermeier, J. Notholt, C.P. Rinsland, H. Schrijver, D. Smale, A. Strandberg, A.G. Straume, W. Stremme, K. Strong, R. Sussmann, J.R. Taylor, M. van den Broek, T. Wagner, T. Warneke, A. Wiacek, and S. Wood. Atmos. Chem. Phys. **6**, 1953 (2006).
20. A. Wiacek, N.B. Jones, K. Strong, J.R. Taylor, R.L. Mittermeier, and H. Fast. Geophys. Res. Lett. **33**, L03811 (2006); doi:10.1029/2005GL024897.
21. E.J. Llewellyn, N.D. Lloyd, D.A. Degenstein, R.L. Gattinger, S.V. Petelina, A.E. Bourassa, J.T. Wiensz, E.V. Ivanov, I.C. McDade, B.H. Solheim, J.C. McConnell, C.S. Haley, C. von Savigny, C.E. Sioris, C.A. McLinden, E. Griffioen, J. Kaminski, W.F.J. Evans, E. Puckrin, K. Strong, V. Wehrle, R.H. Hum, D.J.W. Kendall, J. Matsushita, D.P. Murtagh, S. Brohede, J. Stegman, G. Witt and G. Barnes, W.F. Payne, L. Piché, K. Smith, G. Warshaw, D.L. Deslauniers, P. Marchand, E.H. Richardson, R.A. King, I. Wevers, W. McCreath, E. Kyrölä, L. Oikarinen, G.W. Leppelmeier, H. Auvinen, G. Mégie, A. Hauchecorne and F. Lefèvre, J. de La Nöe, P. Ricaud, U. Frisk, F. Sjoberg, F. von Schéele, and L. Nordh. Can. J. Phys. **82**, 411 (2004).
22. H.L. Nordh, F. von Scheele, U. Frisk, K. Ahola, R.S. Booth, P.J. Encrenaz, A. Hjalmarson and D. Kendall, E. Kyrola, and S. Kwok. Astron. Astrophys. **402**, L21 (2003).
23. C.S. Haley, S.M. Brohede, C.E. Sioris, E. Griffioen, D.P. Murtagh, I.C. McDade, P. Eriksson and E.J. Llewellyn, A. Bazureau, and F. Goutail. J. Geophys. Res. **109**, D16303 (2004); doi:10.1029/2004JD004588.
24. C. von Savigny, C.S. Haley, C.E. Sioris, I.C. McDade, E.J. Llewellyn, D. Degenstein W.F.J. Evans, R.L. Gattinger, E. Griffioen, E. Kyrölä and N.D. Lloyd, J.C. McConnell, C.A. McLinden and G. M/'egie, D.P. Murtagh, B. Solheim, and K. Strong. Geophys. Res. Lett. **30**, 1755 (2003).
25. S.M. Brohede, C.S. Haley, C.A. McLinden, C.E. Sioris, D.P. Murtagh, S.V. Petelina, E.J. Llewellyn, A. Bazureau, F. Goutail, C.E. Randall, J.D. Lumpe, G. Taha, L.W. Thomasson, and L.L. Gordley. J. Geophys. Res. **112**, D07310 (2007); doi:10.1029/2006JDO07586.
26. C. von Savigny, I.C. McDade, E. Griffioen, C.S. Haley, C.E. Sioris, and E.J. Llewellyn. Can. J. Phys. **83**, 957 (2005).
27. S.V. Petelina, E.J. Llewellyn, D.A. Degenstein, N.D. Lloyd, R.L. Gattinger, C.S. Haley, C. von Savigny, E. Griffioen, I.C. McDade, W.F.J. Evans, D.P. Murtagh, and J. de La Noe. Geophys. Res. Lett. **31**, L07104 (2004); doi:10.1029/2003GL019299.
28. S.V. Petelina, E.J. Llewellyn, K.A. Walker, D.A. Degenstein, C.D. Boone, P.F. Bernath, C.S. Haley, C. von Savigny, N.D. Lloyd, and R.L. Gattinger. Geophys. Res. Lett. **32**, L15S06 (2005); doi:10.1029/2005GL022377.
29. C.S. Haley and S.M. Brohede. Can. J. Phys. **85**, This issue (2007).
30. A. Wiacek, J.R. Taylor, K. Strong, R. Saari, T.E. Kerzenmacher, N. Jones, and D.W.T. Griffith. J. Atmos. Oceanic Technol. **24**, 432 (2007).
31. C.P. Rinsland, M.A.H. Smith, P.L. Rinsland, A. Goldman and J.W. Brault, and G.M. Stokes. J. Geophys. Res. **87**, 11119 (1982).
32. N.S. Pougatchev, B.J. Connor, and C.P. Rinsland. J. Geophys. Res. **100**, 16689 (1995).
33. L.S. Rothman, D. Jacquemart, A. Barbe, D.C. Benner, M. Birk, L.R. Brown, M.R. Carleer, C. Chackerian Jr, K. Chance, V. Dana, V.M. Devic, J.-M. Flaud, R.R. Gamache, A. Goldman, J.-M. Hartmann, K.W. Jucks, A.G. Maki, J.-Y. Mandin, S.T. Massie, J. Orphal, A. Perrin, C.P. Rinsland and M.A.H. Smith, J. Tennyson, R.N. Tolchenov, R.A. Tothe and J.V. Auwera, P. Varanasi, and G. Wagner. J. Quant. Spectros. Radiat. Transfer, **96**, 139 (2005).
34. C. Rodgers. Inverse methods for atmospheric sounding: Theory and practice. World Scientific, Singapore. 2004.
35. C. Camy-Peyret, J.M. Flaud, J. Laurent, and G.M. Stokes. Geophys. Res. Lett. **10**, 35 (1983).
36. F. Hase, J.W. Hannigan, M.T. Coffey, A. Goldman, M. Höpfner, N.B. Jones, C.P. Rinsland, and S.W. Wood. J. Quant. Spectros. Radiat. Transfer, **87**, 25 (2004).
37. J.M. Flaud, C. Camy-Peyret, D. Cariolle, J. Laurent, and G.M. Stokes. Geophys. Res. Lett. **10**, 1104

(1983).
38. J.M. Flaud, C. Camy-Peyret, J.W. Brault, C.P. Rinsland, and D. Cariolle. Geophys. Res. Lett. **15**, 261 (1988).
39. M. De Mazière, M. Van Roozendael, C. Hermans, P.C. Simon, P. Demoulin, G. Roland, and R. Zander. J. Geophys. Res. **103**, D16303 (1998); doi:10.1029/97JD03362.
40. J.C. Lambert, T. Blumenstock, F. Boersma, A. Bracher, M. De Mazière, P. Demoulin, I. De Smedt, H. Eskes, M. Gil, F. Goutail, J. Granville, F. Hendrick, D.V. Ionov, P.V. Johnston, I. Kostadinov, K. Kreher, E. Kyrö, R. Martin, A. Meier, E. Navarro-Comas, A. Petritoli, J.P. Pommereau, A. Richter, H.K. Roscoe, C. Sioris, R. Sussmann, M. Van Roozendael, T. Wagner, S. Wood, and M. Yela. *In* Proceedings of ACVE-2 Workshop. Frascati, Italy. May 2004. ESA-ESRIN, Frescati, Italy. 2004.
41. J.M. Russell, L.L. Gordley, L.E. Deaver, R.E. Thompson, and J.H. Park. Adv. Space Res. **14**, 9 (1994).
42. B. Carli, D. Alpaslan, M. Carlotti, E. Castelli, S. Ceccherini, B.M. Dinelli, A. Dudhia, J.M. Flaud, M. Hoepfner, V. Jay, L. Magnani, H. Oelhaf and V. Payne, C. Piccolo, M. Prosperi, P. Raspollini, J. Remedios, M. Ridolfi, and R. Spang. Adv. Space Res. **33**, 1012 (2004).
43. A. Wiacek. Ph.D. thesis, University of Toronto. 2006.
44. M. De Mazière, T. Coosemans, B. Barret, T. Blumenstock, A. Griesfeller, P. Demoulin, H. Fast, D. Griffith, N. Jones, E. Mahieu, J. Mellqvist and R.L. Mittermeier, J. Notholt, C. Rinsland and A. Schulz, D. Smale, A. Strandberg, R. Sussmann, S. Wood, and M. Buchwitz.*In* Proceedings of Envisat Validation Workshop, Frascati, Italy. December 2002. ESA-ESRIN, Frescati, Italy. 2002.
45. A. Griesfeller, J. Griesfeller, F. Hase, T. Blumenstock, and H. Nakajima. *In* American Geophysical Union — Fall Meeting, San Fransisco, USA. December 2005. The American Geophysical Union, San Francisco, USA. 2005.
46. D. Wunch, J.R. Taylor, D. Fu, P. Bernath, J.R. Drummond, C. Midwinter, K. Strong, and K.A. Walker. Atmos. Chem. Phys. **7**, 1275 (2007).
47. U. Frisk, M. Hagström, J. Ala-Laurinaho, S.,ersson and J.-C. Berges, J.-P. Chabaud, M. Dahlgren, A. Emrich, H.-G. Florén, G. Florin, M. Fredrixon, T. Gaier, R. Haas, T. Hirvonen, ÅHjalmarsson, B. Jakobsson, P. Jukkala, P. S. Kildal, E. Kollberg, J. Lassing, A. Lecacheux, P. Lehikoinen, A. Lehto, J. Mallat, C. Marty, D. Michet, J. Narbonne, M. Nexon, M. Olberg, A. O. H. Olofsson, G. Olofsson, A. Origné, M. Petersson, P. Piironen, R. Pons, D. Pouliquen, I. Ristorcelli, C. Rosolen, G. Rouaix, A. V. Räisänen, G. Serra, F. Sjöberg, L. Stenmark, S. Torchinsky, J. Tuovinen, C. Ullberg, E. Vinterhav, N. Wadefalk, H. Zirath, P. Zimmermann, and R. Zimmermann. Astron. Astrophys. **402**, L27 (2003).
48. D. Murtagh, U. Frisk, F. Merino, M. Ridal, A. Jonsson and J. Stegman, G. Witt, P. Eriksson and C. Jiménez, G. Megie, J. de la Noë, P. Ricaud and P. Baron, J.R. Pardo, A. Hauchcorne, E.J. Llewellyn, D.A. Degenstein, R.L. Gattinger, N.D. Lloyd, W.F.J. Evans, I.C. McDade, C.S. Haley and C. Sioris, C. von Savigny, B.H. Solheim, J.C. McConnell, K. Strong, E.H. Richardson, G.W. Leppelmeier, E. Kyrölä, H. Auvinen, and L. Oikarinen. Can. J. Phys. **80**, 309 (2002).
49. D.A. Degenstein, A.E. Bourassa, C.Z. Roth, N.D. Lloyd, and E.J. Llewellyn. *In* American Geophysical Union - Fall Meeting, San Fransisco, USA. December 2006. The American Geophysical Union, San Francisco, USA. 2006.
50. D.E. Flittner, P.K. Bhartia, and B.M. Herman. Geophys. Res. Lett. **27**, 2061 (2000).
51. G. Wetzel, A. Bracher, B. Funke, F. Goutail, F. Hendrick, J.C. Lambert, S. Mikuteit, C. Piccolo, M. Pirre, A. Bazureau, C. Belotti, T. Blumenstock, M. De Mazière, H. Fischer, N. Huret, D. Ionov, M. López-Puertas, G. Maucher, H. Oelhaf, J.P. Pommereau, R. Ruhnke, M. Sinnhuber, G. Stiller, M. Van Roozendael, and G. Zhang. Atmos. Chem. Phys. **7**, 3261 (2007).
52. C.A. McLinden, S.C. Olsen, B. Hannegan, O. Wild, M.J. Prather, and J. Sundet. J. Geophys. Res. **105**, 14653 (2000).
53. H.K. Roscoe, A.J. Charlton, D.J. Fish and J.G.T. Hill. J. Quant. Spectros. Radiat. Transfer, **68**, 337 (2001).
54. C. Rodgers and B.J. Connor. J. Geophys. Res. **108**, D3 (2003); doi:10.1029/2002JD002299.
55. A.C. Vandaele, C. Fayt, F. Hendrick, C. Hermans, F. Humbled, M. Van Roozendael, M. Gil, M. Navarro, O. Puentedura, M. Yela, G. Braathen, K. Stebel, K. Tørnkvist, P. Johnston, K. Kreher, F. Goutail, A. Mieville, J.-P. Pommereau, S. Khaikine, A. Richter, H. Oetjen, F. Wittrock, S. Bugarski, U. Frieß, K. Pfeilsticker, R. Sinreich, T. Wagner, G. Corlett, and R. Leigh. J. Geophys. Res. **110**, D08305 (2005); doi:10.1029/2004JD005423.

56. A.C. Vandaele, C. Hermans, P.C. Simon, M. Carleer, R. Colin, S. Fally, M.F. Merienne, A. Jenouvrier, and B. Coquart. J. Quant. Spectros. Radiat. Transfer, **59**, 171 (1998).
57. A. Perrin, J.-M. Flaud, A. Goldman, C. Camy-Peyret, W.J. Lafferty, P. Arcas, and C.P. Rinsland. J. Quant. Spectros. Radiat. Transfer, **60**, 839 (1998).
58. M. Palm, C. von Savigny, T. Warneke, V. Velazco, J. Notholt, K. K$^{'}$unzi, J. Burrows, and O. Schrems. Atmos. Chem. Phys. Diss. **5**, 911 (2005).
59. K. Bogumil, J. Orphal, T. Homann, S. Voigt, P. Spietz, O.C. Fleischmann, A. Vogel, M. Hartmann, H. Kromminga, H. Bovensmann, J. Frerick, and J.P. Burrows. J. Photochem. Photobiol. A: Chem. **157**, 167 (2003).
60. S. Mikhailenko, A. Barbe, and V.G. Tyuterev. J. Mol. Spec. **215**, 29 (2002).
61. M.R. De Backer-Barilly, A. Barbe, and V.G. Tyuterev. Atmos. Oceanic Opt. **16**, 183 (2003).